



Cite this: *Dalton Trans.*, 2022, **51**, 10357

Received 14th February 2022,
Accepted 4th June 2022

DOI: 10.1039/d2dt00458e

rsc.li/dalton

Luminescent early-late-hetero-tetranuclear group IV – Au(I) bisamidinate complexes†

Cedric Uhlmann,^a Thomas J. Feuerstein,^a Tim P. Seifert,^a André P. Jung,^a Michael T. Gamer,^a Ralf Köppe,^a Sergei Lebedkin,^b Manfred M. Kappes^{b,c} and Peter W. Roesky^a★

The versatile metalloligand $[(\text{HC}\equiv\text{CC}(\text{NDipp})_2)_2\text{Au}_2]$ (dipp = 2,6-diisopropylphenyl) was converted into early-late heterotetrametallic complexes $[(\text{ClCp}_2\text{MC}\equiv\text{CC}(\text{NDipp})_2)_2\text{Au}_2]$ (M = Ti, Zr). These compounds show photoluminescence with either remarkably different (Ti) or similar (Zr) features as compared to related solely coinage metal containing acetylide amidinate complexes.

Complexes that contain both early and late transition metals, so-called early-late heterobimetallics (ELHBs), have been of particular interest for quite some time^{1,2} and have become a constantly growing research topic.^{3,4} The main reason for this interest is their potential utility in homogeneous catalysis, since the pairing of electronically different metal cores in one complex may lead to cooperative effects.^{3,4} Such electronic communication is thought to play a role in heterogeneous catalysts, for instance, in those containing late transition metals like Au which are dispersed on Lewis acidic supports like TiO_2 . These catalysts often show increased catalytic activity in comparison to their precious metal free congeners.⁵

This increase is attributed to the electronic interaction between the electron-poor and electron-rich metal atoms and their substrate activation *via* different coordination sites.⁶ However, detailed evidence for this phenomenon is scarce and such cooperative interactions are not well understood so far. Hence, the assembly of two electronically different metals within one complex can act as a model system to investigate intermetallic communication and cooperative behaviour with respect to luminescent or catalytic properties.⁷

The synthesis of early-late heterobimetallic complexes (ELHBs) in principle requires a ligand system, which combines

different donor sites with an affinity for the electron deficient and electron rich metal atoms, respectively.^{8–10} This is, for example, a combination of a hard donor centre like an alkoxide and a soft donor centre like a phosphine.^{11,12} However, by a stepwise complex synthesis and utilization of metalloligands, it is also possible to use ligands providing donor sites with an affinity for both metal atoms. This requires that the first implemented metal is sufficiently stabilized by the ligand system. Such condition can be realized, for instance, with functionalized alkynes.¹³

From a photophysical point of view, interesting metals regarding the synthesis of ELHBs include gold and zirconium. Indeed, gold(I) complexes are well known for effective phosphorescence due to the heavy atom effect which can be further modulated by metallophilic interactions.^{14–20} Zirconium(IV) complexes, particularly derivatives exhibiting cyclopentadienyl ligands,²¹ often show distinct PL in the visible spectral range as well.²²

Herein we report on the successful application of ethynylamidinates for the synthesis of tetranuclear group IV – gold(I) ELHB complexes. Since gold(I) amidinates come along with short, fully supported aurophilic interactions²³ and the implemented ligand system furthermore exhibits a conjugated π -system which bridges the early and late metal atoms, the group IV – gold(I) ELHB compounds represent promising objects for photophysical studies. Following our previously published reaction protocol, at first, the complex $[(\text{HC}\equiv\text{CC}(\text{NDipp})_2)_2\text{Au}_2]$ was lithiated *in situ* with two equivalents of *n*-butyllithium at -78°C in tetrahydrofuran.²⁴ Subsequently, two equivalents of the precursors Cp_2MCl_2 (M = Ti, Zr) were added to obtain the complexes $[(\text{ClCp}_2\text{MC}\equiv\text{CC}(\text{NDipp})_2)_2\text{Au}_2]$, **1** (M = Ti) and **2** (M = Zr) (Scheme 1). Compound **1** was obtained in form of a dark red solid. Remarkably, the dried compound is air stable over at least one month. In comparison to the starting material, in the ^1H NMR spectrum of **1**, similar resonances for the protons belonging to the 2,6-diisopropylphenyl (Dipp) moieties are observed.

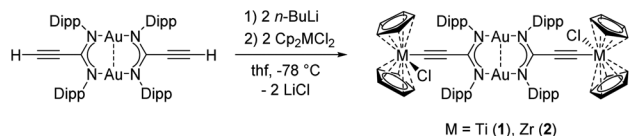
As expected, no resonance was detected in the range of the terminal alkyne protons and, a singlet arises for the cyclopent-

^aInstitute for Inorganic Chemistry, Karlsruhe Institute of Technology (KIT), Engesserstr. 15, 76131 Karlsruhe, Germany. E-mail: roesky@kit.edu

^bInstitute of Nanotechnology, Karlsruhe Institute of Technology (KIT), Hermann-von-Helmholtz-Platz 1, 76344 Eggenstein-Leopoldshafen, Germany

^cInstitute of Physical Chemistry, Karlsruhe Institute of Technology (KIT), Fritz-Haber-Weg 2, 76131 Karlsruhe, Germany

† Electronic supplementary information (ESI) available. CCDC 2151930–2151931. For ESI and crystallographic data in CIF or other electronic format see DOI: <https://doi.org/10.1039/d2dt00458e>



Scheme 1 Synthesis of the compounds $[\{\text{ClCp}_2\text{TiC}\equiv\text{CC}(\text{NDipp})_2\}_2\text{Au}_2]$ (**1**) and $[\{\text{ClCp}_2\text{ZrC}\equiv\text{CC}(\text{NDipp})_2\}_2\text{Au}_2]$ (**2**).

tadienyl protons at $\delta = 5.66$ ppm. Furthermore, the Cp-carbon atoms are detected at $\delta = 116.2$ ppm as the most intense resonance in the $^{13}\text{C}\{^1\text{H}\}$ NMR spectrum of **1**. The alkyne carbon atoms are detected at $\delta = 154.8$ and 120.2 ppm. These are significantly shifted in comparison to $[\{\text{HC}\equiv\text{CC}(\text{NDipp})_2\}_2\text{Au}_2]$ (89.1 and 75.8 ppm) and comparable to the chemical shifts for $[\{\text{PPh}_3\}\text{AuC}\equiv\text{CC}(\text{NDipp})_2\}_2\text{Au}_2]$ (155.3 and 123.7 ppm).²⁴ Moreover, in the IR spectrum of **1** only a very weak band appears in the range of $\text{C}\equiv\text{C}$ bonds, but a very strong vibrational mode is detected at $\nu(\text{C}\equiv\text{C}) = 2088\text{ cm}^{-1}$ in the Raman spectrum. Single crystals suitable for X-ray analysis of compound **1** were obtained in form of red prisms. The complex crystallizes in the triclinic space group $P\bar{1}$ featuring an inversion centre in the centre of the molecule in between the Au atoms. The titanium atoms in the molecular structure of **1** in the solid state (Fig. 1) are terminally coordinated to the acetylide moieties. The Ti1–C3–C2 angle of $175.1(8)^\circ$ is near to the ideal value of 180° . The Cl1–Ti1–C3 angle of $95.4(2)^\circ$ and the Ti1–C3 bond length of $2.100(6)\text{ \AA}$ are in consistency with similar compounds.²⁵ The Ti–Cl as well as the Ti–Cp distances are comparable to the starting material Cp_2TiCl_2 .²⁶ The central structural motif, which consists of two NCN units and two gold(i) ions, only shows insignificant deviations from the parent compound and the $\text{C}\equiv\text{C}$ bond length C2–C3 of $1.210(8)\text{ \AA}$ is in the typical range for a C–C triple bond. The zirconium complex $[\{\text{ClCp}_2\text{ZrC}\equiv\text{CC}(\text{NDipp})_2\}_2\text{Au}_2]$ (**2**) was obtained as a yellow solid after a similar work-up as for **1**. In contrast to **1**, however, **2** is extremely sensitive to moisture and

partially gets hydrolyzed to yield the starting material $[\{\text{HC}\equiv\text{CC}(\text{NDipp})_2\}_2\text{Au}_2]$ and the zirconium bridged oxide $(\text{Cp}_2\text{ZrCl})_2\mu\text{-O}$. The measured unit cell was in accordance with literature²⁷ and the NMR-spectra showed only the starting material $[\{\text{HC}\equiv\text{CC}(\text{NDipp})_2\}_2\text{Au}_2]$ as shown in our previous work.²⁴ In consistency with **1**, the ^1H NMR spectrum of the Zr complex **2** also shows no resonance for terminal alkyne protons. Therefore, a distinct singlet resonance appears for the cyclopentadienyl protons at $\delta = 5.46$ ppm. In the $^{13}\text{C}\{^1\text{H}\}$ NMR spectrum the corresponding Cp–CH resonance is observed at $\delta = 113.2$ ppm, while the alkyne carbon atoms are detected at $\delta = 149.3$ and 115.8 ppm. The IR and Raman spectra appear very similar to the spectra of **1**. However, the stretching mode of the $\text{C}\equiv\text{C}$ bonds at $\tilde{\nu}(\text{C}\equiv\text{C}) = 2094\text{ cm}^{-1}$ in the Raman spectrum of **2** is slightly shifted to higher wavenumbers in comparison with **1**. Single crystals of compound **2** were obtained from toluene/*n*-pentane. Thereby the compound crystallizes analogously to **1** in the triclinic space group $P\bar{1}$ (Fig. 2).

The asymmetric unit contains half of a molecule with a crystallographic inversion centre in the middle of the two gold atoms. Like for complex **1**, a terminal acetylide–metal coordination with a Zr1–C3–C2 angle of $178.6(6)^\circ$ is observed. The Cl1–Zr1–C3 angle of $99.7(2)^\circ$ as well as the Zr1–C3 bond length of $2.236(6)\text{ \AA}$ are expectedly slightly larger in comparison to **1**. All parameters for the central motif are in consistency with the starting material²⁴ and the C2–C3 bond length of $1.193(8)\text{ \AA}$ is still in the typical range for a $\text{C}\equiv\text{C}$ triple bond.

Subsequently, we also intended to synthesize an analogous hafnium compound. However, although the colour and luminescence of the reaction solution appeared like those for complex **2**, we were not able to isolate a neat product.

Following the synthesis and characterization, we thoroughly investigated the PL behaviour of **1** and **2** in the solid (polycrystalline) state at variable temperatures between 20 and 295 K. Of particular interest was the influence of the group 4 metallocene chloride moieties on the PL properties with regard to the

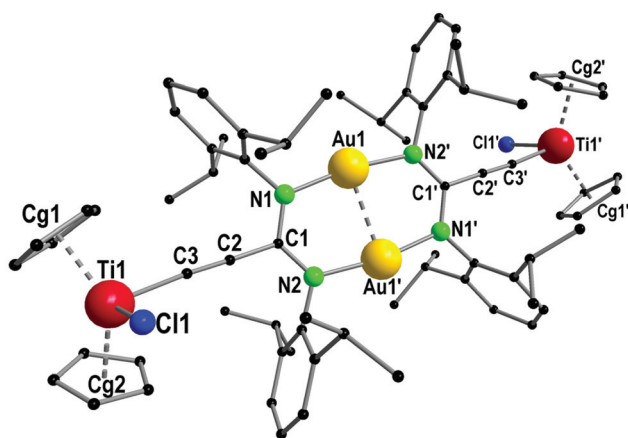


Fig. 1 Molecular structure of compound **1** in the solid state. Hydrogen atoms are omitted for clarity. Structural parameters are given in the ESI.† (Cg = ring centroid).

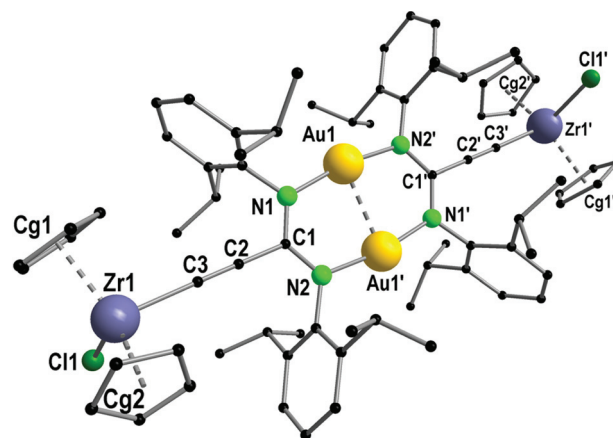


Fig. 2 Molecular structure of compound **2** in the solid state. Hydrogen atoms are omitted for clarity. Structural parameters are given in the ESI.† (Cg = ring centroid).



closely related di- and tetranuclear gold(i) bisethynylamidinate complexes we recently reported.²⁴

The zirconium complex **2** emits bright yellow phosphorescence with the maximum at 545 nm (Fig. 3 and Table 1), high quantum yield $\Phi_{\text{PL}} = 41\%$ and lifetime of 5.9 μs at ambient temperature (Fig. S13 and Table S2†). Its intensity moderately increases upon cooling to 20 K (with $\Phi_{\text{PL}} \approx 60\%$ as estimated from the temperature-dependent PL spectra), roughly correlating to the increased PL lifetime (9.8 μs). These PL properties are similar to those of the related di- and tetranuclear gold(i) bisethynylamidinates,²⁴ with the exception of a *ca.* 50 nm blueshift of the emission and PL excitation (PLE) onset observed for the latter.

In contrast, absorption and phosphorescence of the titanium complex **1** are strongly redshifted clearly indicating the influence of the group 4 metal coordinated to the acetylide function. The PLE onset at *ca.* 620 nm corresponds to a dark red visual appearance of the solid compound. Such increase of the energy gap from Ti to Zr (and further to Hf) appears to be common for homologous complexes with the lowest unoccupied molecular orbitals (MOs) mainly contributed by d orbitals of these metals (see below).²⁸ The red emission of **1** has a maximum at 720/705 nm (at 20/295 K), decays on a sub-micro-second timescale (Fig. S13†) and shows a quantum efficiency of only 0.6% at ambient temperature (Table S2†). The different emission colours of **1** and **2** are illustrated in the CIE 1931 diagram (Fig. S14†). In addition, complex **1** features a rare type of temperature dependence of the (integral) PL intensity, moderately decreasing upon cooling below 250 K (Fig. 3). These observations suggest that the PL properties of **1** are crucially determined by the titanocene terminal moieties.

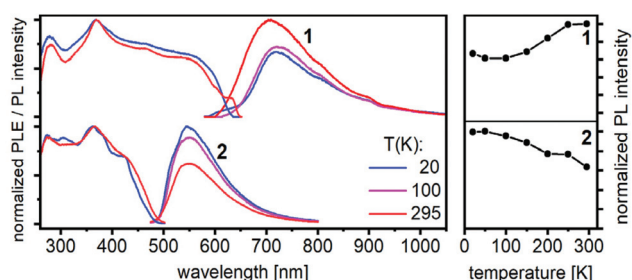


Fig. 3 Left: Normalized photoluminescence excitation (PLE) and emission (PL) spectra of compounds **1** and **2** at 20, 100 and 295 K. The PL/PLE spectra were excited/recorded at 350/710 nm (**1**) and 360/550 nm (**2**). Right: The integral PL intensity vs. temperature.

Table 1 Absorption onset and emission maximum for solid compounds **1**, **2** and the binuclear Au_2 precursor complex $[(\text{HC}\equiv\text{CC}(\text{NDipp})_2)_2\text{Au}_2]$ (ref. 24)

| Compound | Absorption (nm) 295 K | Emission (nm) 20/295 K |
|---------------------------------------|-----------------------|------------------------------------|
| Au_2 | 430 | 500 ^a /490 ^a |
| Ti_2Au_2 (1) | 620 | 720/705 |
| Zr_2Au_2 (2) | 490 | 545/550 |

^a Centre wavelength.

The similarities and differences between **1**, **2** and the related tetranuclear gold(i) bisethynylamidinate complex $[(\text{PPh}_3)\text{AuC}\equiv\text{CC}(\text{NDipp})_2]_2\text{Au}_2$ ²⁴ were further elucidated by DFT calculations (for details see the ESI†). The character of the triplet (emitting) state is similar in **1** and **2**, but distinct in the Au_2Au_2 complex. The non-relaxed density plots reveal excitations predominantly promoted by occupied MOs of the Au_2N_4 core and unoccupied d orbitals of Ti and Zr in **1** and **2**, whereas a contribution of the terminal Au atoms in the Au_4 complex is negligible, only unoccupied MOs of the phosphine terminal groups are involved (Fig. 4). The different characters of the triplet state may have connection with the observation of vibronically well-structured emission of the Au_2Au_2 complex,²⁴ whereas this is absent in **1** and **2** (Fig. 3). Namely, the vibronic coupling might be contributed by the phosphine groups in the former compound. The calculations underestimated the emission (phosphorescence) energies by about 0.3 eV for **1** and Au_2Au_2 complexes and by 0.5 eV for **2** as compared with the experimental values obtained for solid (crystal-line) samples (Table S3†). A trend of the relative emission is, however, reproduced much better, within 0.2 eV.

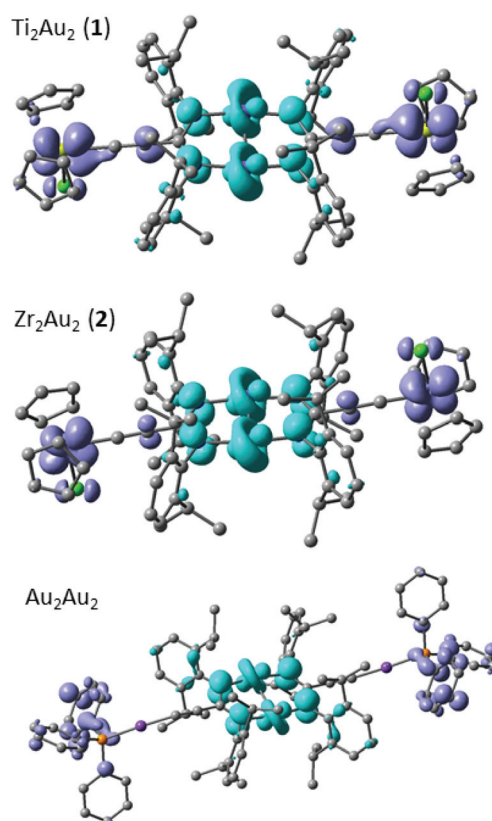


Fig. 4 Non-relaxed transition densities calculated for the T_1 triplet excitations of tetranuclear Ti_2Au_2 (**1**) and Zr_2Au_2 (**2**) complexes in comparison to the structurally related tetranuclear gold(i) bisethynylamidinate $[(\text{Ph}_3\text{PAu}_2\text{MC}\equiv\text{CC}(\text{NDipp})_2)_2\text{Au}_2]$.²⁴ The contributions of occupied orbitals are plotted in pale blue and those of unoccupied orbitals in violet.

Conclusions

Two new early-late heterobimetallic complexes $[\{\text{ClCp}_2\text{MC}\equiv\text{CC}(\text{NDipp})_2\}_2\text{Au}_2]$ ($\text{M} = \text{Ti}, \text{Zr}$) and their photophysical characteristics are presented. This was achieved *via* direct lithiation of a previously used ethynyl compound $[\{\text{HC}\equiv\text{CC}(\text{NDipp})_2\}_2\text{Au}_2]$ followed by the reaction with Cp_2MCl_2 ($\text{M} = \text{Ti}, \text{Zr}$). The heavier hafnium analogue could not be isolated, even after several attempts.

The zirconium complex emits yellow phosphorescence with quantum yields of 41% in the solid state under ambient temperature and 60% upon cooling to 20 K. In contrast, the titanium complex emits red phosphorescence with a quantum yield of only 0.6% at ambient conditions. Additionally, it features a rare type of the temperature dependence of the PL intensity, moderately decreasing upon cooling below 250 K.

This distinction in the otherwise structurally very similar compounds is likely due to the different electronic interaction between the group IV metals and the gold(I) moieties as indicated by the TDDFT calculations. Along similar lines, substitution of the remaining chloride atom on the group IV metal may lead to a series of compounds with adjustable photoluminescent properties and therefore could bring more insight into the role of metal-metal interactions in determining the photoluminescent behaviour of early-late-heterobimetallic complexes.

Experimental section

Experimental details are found in the ESI.†

Conflicts of interest

There are no conflicts to declare.

Acknowledgements

Financial support by the DFG funded transregional collaborative research centre SFB/TRR 88 "Cooperative Effects in Homo and Heterometallic Complexes (3MET)" is gratefully acknowledged (projects C1 and C7). The authors acknowledge support by the state of Baden-Württemberg through bwHPC and the German Research Foundation (DFG) through grant no INST 40/575-1 FUGG (JUSTUS 2 cluster).

Notes and references

- 1 D. W. Stephan, *Coord. Chem. Rev.*, 1989, **95**, 41–107.
- 2 N. Wheatley and P. Kalck, *Chem. Rev.*, 1999, **99**, 3379–3420.
- 3 P. Buchwalter, J. Rosé and P. Braunstein, *Chem. Rev.*, 2015, **115**, 28–126.
- 4 E. Bodio, M. Picquet and P. Le Gendre, in *Homo- and Heterobimetallic Complexes in Catalysis: Cooperative Catalysis*, ed. P. Kalck, Springer International Publishing, Cham, 2016, pp. 139–186. DOI: [10.1007/978-3-319-21511-1_161](https://doi.org/10.1007/978-3-319-21511-1_161).
- 5 S. J. Tauster, *Acc. Chem. Res.*, 1987, **20**, 389–394.
- 6 S. S. Langer, E. Chatt, B. T. Heaton, D. M. P. Mingos, J. R. Dilworth, C. D. Garner, G. Frenking, R. L. Richards, G. A. Gamlen and J. Lewis, *Modern Coordination Chemistry: The Legacy of Joseph Chatt*, Royal Society of Chemistry, Cambridge, 2007.
- 7 U. Helmstedt, S. Lebedkin, T. Höcher, S. Blaurock and E. Hey-Hawkins, *Inorg. Chem.*, 2008, **47**, 5815–5820.
- 8 P. Braunstein and F. Naud, *Angew. Chem., Int. Ed.*, 2001, **40**, 680–699.
- 9 S. Fritzsche, P. Lönnecke, T. Höcher and E. Hey-Hawkins, *Z. Anorg. Allg. Chem.*, 2006, **632**, 2256–2267.
- 10 F. Völcker, F. M. Mück, K. D. Vogiatzis, K. Fink and P. W. Roesky, *Chem. Commun.*, 2015, **51**, 11761–11764.
- 11 R. Ruiz, J. Faus, F. Lloret, M. Julve and Y. Journaux, *Coord. Chem. Rev.*, 1999, **193–195**, 1069–1117.
- 12 S. Bestgen, C. Schöo, C. Zovko, R. Köppe, R. P. Kelly, S. Lebedkin, M. M. Kappes and P. W. Roesky, *Chem. – Eur. J.*, 2016, **22**, 7115–7126.
- 13 V. Fernández-Moreira, I. Marzo and M. C. Gimeno, *Chem. Sci.*, 2014, **5**, 4434–4446.
- 14 M. Olaru, J. F. Kögel, R. Aoki, R. Sakamoto, H. Nishihara, E. Lork, S. Mebs, M. Vogt and J. Beckmann, *Chem. – Eur. J.*, 2020, **26**, 275–284.
- 15 H. Schmidbaur and A. Schier, *Chem. Soc. Rev.*, 2012, **41**, 370–412.
- 16 H. Schmidbaur and A. Schier, *Chem. Soc. Rev.*, 2008, **37**, 1931–1951.
- 17 V. W.-W. Yam and E. C.-C. Cheng, *Chem. Soc. Rev.*, 2008, **37**, 1806–1813.
- 18 J. M. López-de-Luzuriaga, M. Monge and M. E. Olmos, *Dalton Trans.*, 2017, **46**, 2046–2067.
- 19 T. P. Seifert, V. R. Naina, T. J. Feuerstein, N. D. Knöfel and P. W. Roesky, *Nanoscale*, 2020, **12**, 20065–20088.
- 20 V. R. Naina, F. Krätschmer and P. W. Roesky, *Chem. Commun.*, 2022, **58**, 5332–5346.
- 21 G. V. Loukova and V. A. Smirnov, *Chem. Phys. Lett.*, 2000, **329**, 437–442.
- 22 L. Kuhlmann, R. Methling, J. Simon, B. Neumann, H.-G. Stammer, C. A. Strassert and N. W. Mitzel, *Dalton Trans.*, 2018, **47**, 11245–11252.
- 23 T. J. Feuerstein, M. Poß, T. P. Seifert, S. Bestgen, C. Feldmann and P. W. Roesky, *Chem. Commun.*, 2017, **53**, 9012–9015.
- 24 T. J. Feuerstein, T. P. Seifert, A. P. Jung, R. Müller, S. Lebedkin, M. M. Kappes and P. W. Roesky, *Chem. – Eur. J.*, 2020, **26**, 16676–16682.
- 25 H. Lang, S. Blau, H. Pritzkow and L. Zsolnai, *Organometallics*, 1995, **14**, 1850–1854.
- 26 A. Clearfield, D. K. Warner, C. H. Saldarriaga-Molina, R. Ropal and I. Bernal, *Can. J. Chem.*, 1975, **53**, 1622–1629.
- 27 J. T. Spletstoser, J. M. White, A. R. Tunoori and G. I. Georg, *J. Am. Chem. Soc.*, 2007, **129**, 3408–3419.
- 28 X. Wang, L. Chen, A. Endou, M. Kubo and A. Miyamoto, *J. Organomet. Chem.*, 2003, **678**, 156–165.

